ELSEVIER

Thermochimica Acta 245 (1994) 207-217

thermochimica
acta

Phase diagram determination of II–VI semiconductors ☆

J.C. Tedenac [a,*], J. Jun [b], S. Krukowski [b], M. Bockowski [b], S. Porowski [b], M.C. Record [a], R.M. Ayral-Marin [a], G. Brun [a]

[a] *Laboratoire de Physicochimie des Matériaux Solides – URA 0407, Universite de Montpellier II Sciences et Techniques du Languedoc, 34095 Montpellier Cedex 05, France*

[b] *High Pressure Research Center, Polish Academy of Sciences, Sokolowska 29/37, 01-142 Warsaw, Poland*

Abstract

The application of high pressure DTA to the study of solid–solid and liquid–solid transitions is critically assessed. Pressure–temperature ($p-T$) phase diagrams of mercury chalcogenides (HgS, HgSe and HgTe), for pressures up to 2 GPa, are presented and discussed. The pressure influence on the zinc blende–cinnabar transition is elucidated. A phase transition mechanism is proposed that explains the origin of the hysteresis observed in DTA experiments.

Keywords: Chalcogenide; Cinnabar; DTA; Hysteresis; Mechanism; Phase transition; Semiconductor; Zinc blende

---

1. Introduction

At normal temperature and under high hydrostatic pressure, tetrahedrally coordinated semiconductors (i.e. zinc blende or wurtzite lattice) undergo the transition to white tin (less ionic compounds) or rocksalt (more ionic compounds) structures. Mercury chalcogenides (HgS, HgSe, HgTe), however, display a different transition sequence: in HgTe and HgSe the transition from zinc blende to cinnabar, to

---

☆ Presented at the Czechoslovak–French–Polish Conference on Calorimetry and Experimental Thermodynamics: Applications to Contemporary Problems, Prague, Czech Republic, 4–7 September 1993.

* Corresponding author.

SSDI 0040-6031(94)01813-V

rocksalt and then to β-Sn structure was observed in pressures up to 40 Gpa [1,2]. The crystallographic symmetry of the intermediate pressure phase of HgSe and HgTe was determined to be cinnabar by Kafalas et al. [3] and Jayaraman et al. [4].

The HgS cinnabar phase (α-HgS) is stable at ambient pressure and temperature; it undergoes the transition to rocksalt structure at pressures close to 30 GPa [2]. Finally, at very high pressures, all semiconductors would transform to a dense packed regular crystallographic structure.

High temperature parts of $p-T$ diagrams of mercury chalcogenides have not been studied intensively until recently [5-8]; hence pressure-temperature ($p-T$) phase diagrams of mercury chalcogenides were known only schematically [4,9,10]. Using zinc blende-cinnabar transition pressures at normal temperatures, obtained by the volume-discontinuity method (they were 0.8 ± 0.3 and 1.4 ± 0.1 GPa for HgSe and HgTe, respectively [4]) and melting temperatures from DTA experiments, Jayaraman et al. [4] proposed a $p-T$ phase diagram for HgTe. Unfortunately, the pressures of HgSe and HgTe transitions were obtained by Jayaraman et al. [4] in a solid state apparatus with a large error of pressure measurement (of the order of 0.1 GPa) and large deviation from hydrostatic conditions in the solid medium. Additionally, the hysteresis of the solid-solid transition was significant and depended on the transition temperature. The authors concluded that the transition is diffusion controlled which was in disagreement with the earlier report of Bridgman [11]. Thus proper determination of these phase diagrams requires the use of hydrostatic high pressure apparatus (with fluid medium) and careful evaluation of the results of thermal experiments.

At normal pressure, α-HgS undergoes the transition to zinc blende at 613 K and the transition entails a large volume change (molar volume change $\Delta V = 1.753$ cm^3). Upon further heating HgS sublimation occurs at normal pressure at 853 K.

Our earlier results established the zinc blende-liquid coexistence line for HgS [7,8], HgSe [5] and HgTe [6] with good accuracy. Unfortunately, it turned out that triple point pressures are much higher than previously reported [4], close to technical limit of our apparatus (2 GPa). Due to errors associated with metastabilities close to the triple points, the coexistence lines (cinnabar-liquid) were not established with good accuracy. Now we summarize our recent results on the pressure dependence of melting temperature of the cinnabar phases of HgSe and HgS, close to their triple points.

Additionally, using HgS data, we analyze the problem of temperature dependence of the hysteresis in solid-solid transition, crucial in determining interphase equilibria by the DTA dynamic method. Since the temperature of the s-s transition for HgS spans from 613 K to 1163 K, we were able to study this dependence over a considerable temperature range.

2. Experimental

The DTA experiments were performed by the use of a high pressure apparatus, which has been described previously [12]. Therefore we will not discuss this design here.

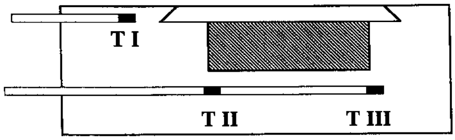

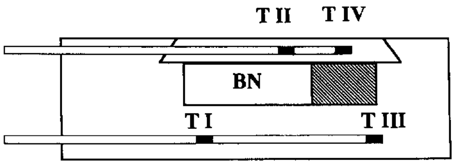

Fig. 1 (left). Scheme of the crucible used in the one zone furnace. TI, control thermocouple; TII and TIII, signal thermocouples.

Fig. 2 (right). Scheme of the crucible used in the three zone furnace. TI, TII and TIV, control thermocouples; TIII, signal thermocouple.

Two different furnace types were used: one zone and three zone. The one zone furnace had been used in earlier DTA experiments. This design inevitably entails thermal gradients in the sample. Therefore, three thermocouples were used in the experiment: T1 for the temperature control, T2 and T3 for the detection of melting and solidification at the high and low temperature ends of the sample. Their location in the crucible is depicted in Fig. 1. The thermal gradient along the crucible can be minimized by proper choice of the location of the crucible in the heater. In our experiments the measured temperature differences were not higher than 40 K.

The three zone furnace was developed in the course of the work reported here. It consists of three independently powered graphite heaters. The arrangement of three control thermocouples (T1, T2 and T3) and the fourth or signal (T4) thermocouple, located close to the sample, is shown in Fig. 2. The setup allows all control thermocouples to be kept within 1 K distance while the signal thermocouple shows the temperature that is not more than 10 K different from the others. This difference, which partially stems from high heating rates, is of order of the temperature differences in the sample during DTA experiments. A comparison of the results obtained in the one and three zone furnaces for the same compound (HgTe) will be given in Section 3.

3. Heating and cooling runs

The heating and cooling rates were optimized so that they were fast enough to observe the latent heat effects (DTA peaks) and did not produce excessive thermal gradients in the sample. The latent heat of the solid–solid transition is several times smaller than that of melting; hence the limit of the heating/cooling rate was in fact determined by the magnitude of the solid–solid transition peak. In Figs. 3–5, we have shown that the signal-control thermocouple temperature difference ΔT, measured during heating and cooling runs.

3.1. HgTe

DTA runs were performed in both configurations. In Fig. 3(a) and (b), we present cooling and heating runs for $p = 0.96$ GPa for the one and three zone

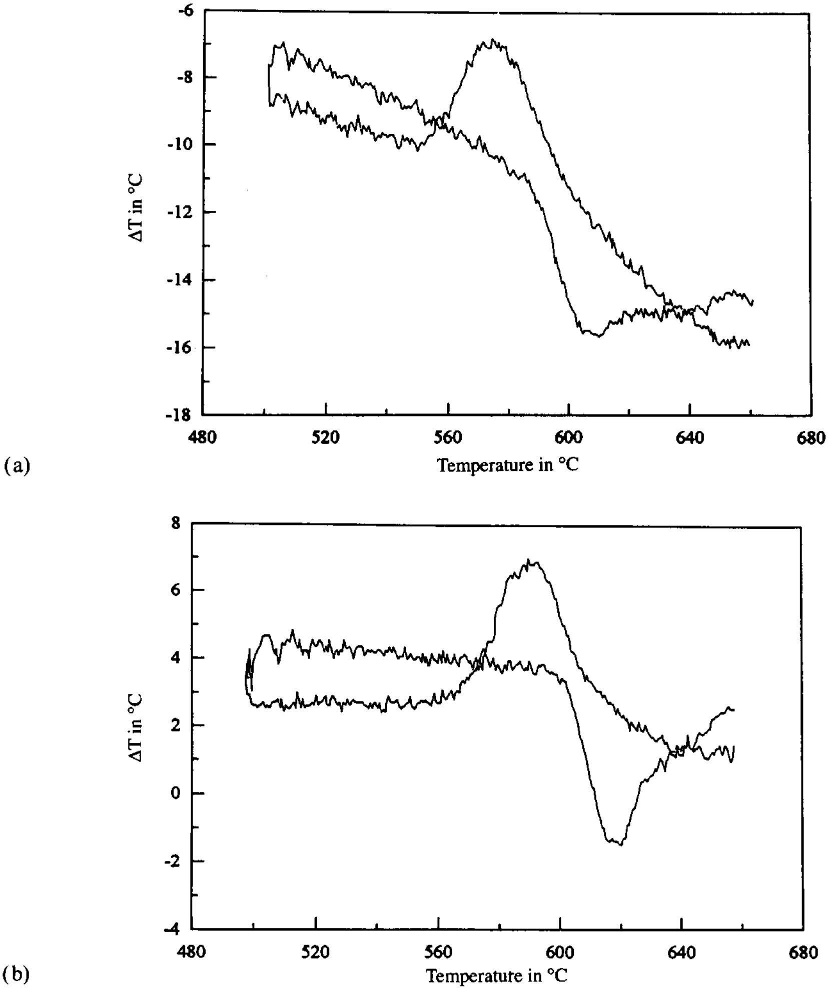

Fig. 3. The temperature difference (TIII – TI) vs. TI, during a heating/cooling run for HgTe for 0.96 GPa: (a) one zone furnace; (b) three zone furnace (temperatures are in °C).

furnace, respectively. The rate was equal to 50 K min^{-1}. In both cases latent heat peaks of magnitude approximately 4 K are clearly distinguishable from the noise. The beginning of the melting peak for the one zone furnace is shifted by about 10 K with respect to the three zone result. The shift is due to the thermal gradient in the sample in the zone furnace; thus the measured temperature is lower than the transition temperature. The existence of the temperature gradients is corroborated by the evolution of ΔT in the run (Fig. 3(a)): for higher temperatures ΔT is larger, due to steeper gradients for higher temperatures. ΔT is much smaller for the three zone furnace (Fig. 3(b)) and its variation during the run is almost unobservable outside the peak area.

3.2. HgSe

The runs of 0.95 and 1.75 GPa are demonstrated in Fig. 4(a) and 4(b). The heating/cooling runs for 0.95 GPa have one peak each, due to melting/solidification. The solid–solid transition is not observed because the transition temperature is lower than the lowest temperature in the run (973 K). The heating and cooling runs for 1.75 GPa (one zone furnace) have two peaks due to zinc blende–cinnabar and cinnabar–liquid transitions. The difference between the beginning of solidification and melting peaks is negligible suggesting the absence of supercooling. On the

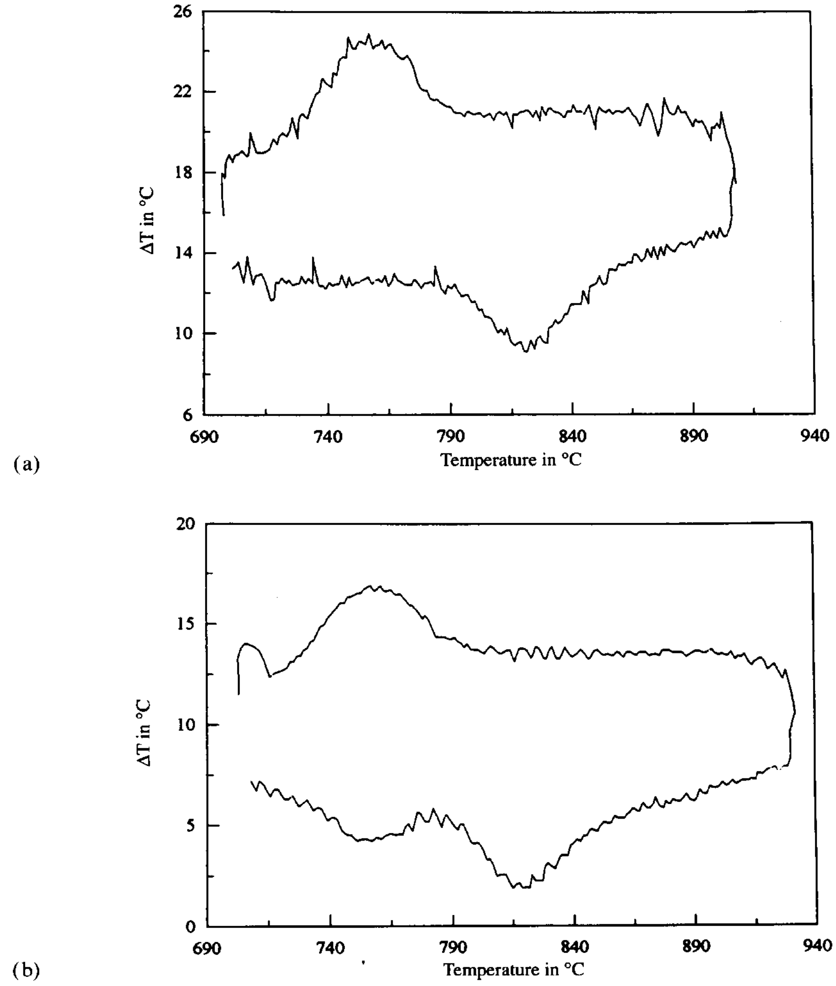

Fig. 4. The temperature difference (TIII – TI) vs. TI, during a heating/cooling run for HgSe: (a) for 0.95 GPa in the three zone furnace; (b) for 1.75 GPa in the one zone furnace (temperatures are in °C).

contrary, the hysteresis in the solid–solid transition leads to a 40 K difference in the transition temperature in heating and cooling runs.

3.3. HgS

The thermal runs for HgS for pressures equal to 1.17 and 1.99 GPa are presented in Fig. 5(a) and (b), respectively. Because of the small heat of the s–s transition, the temperature rate was increased to 60 K min^{-1}. The temperature difference was of the order of 25 K, presumably due to gradients in the sample. For 1.17 GPa, the

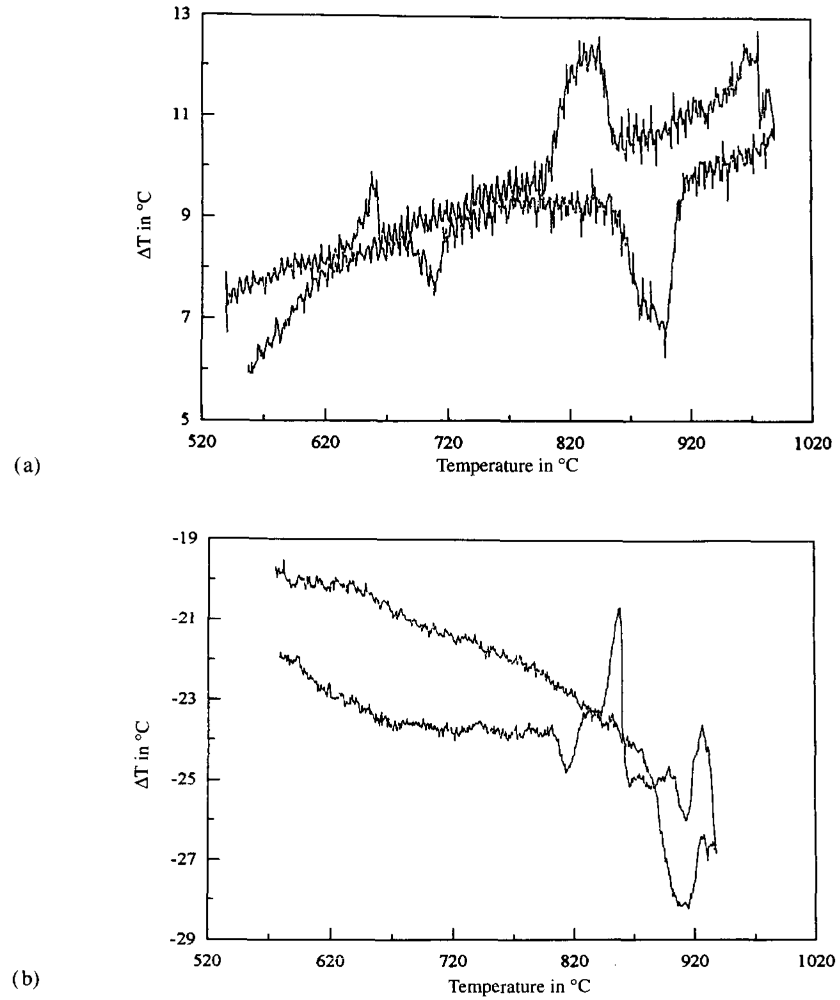

Fig. 5. The temperature difference (TIII – TI) vs. TI, during a heating/cooling run in the three zone furnace for HgS: (a) for 1.17 GPa, (b) for 1.99 GPa (temperatures are in °C).

solid–liquid transition was detected without any noticeable temperature difference whereas the s–s transition showed hysteresis of about 30 K. The cinnabar–zinc blende transition is more diffuse than the solid–solid transition in the opposite direction. For pressure 1.99 GPa, the solidification peak has an additional slope break, probably due to the zinc blende–cinnabar transition.

4. Pressure–temperature ($p-T$) phase diagrams

The resulting $p-T$ phase diagrams are drawn in Fig. 6 ((a) HgTe, (b) HgSe and (c) HgS).

4.1. HgTe

The melting curve for zinc blende of the $p-T$ HgTe diagram is a virtually straight, descending line, indicating the higher density of the liquid. The line shape suggests that the compressibilities of zinc blende and liquid are similar. The triple point ($p = 1.6$ GPa, $T = 832$ K) is observed for much higher pressure than the values reported by Jayaraman et al. [4] and Omel'chenko and Soshnikov [9]. The difference is caused by nonhydrostatic effects which lead to higher pressures in part of the sample in the experiments of Jayaraman et al. [4].

For higher pressures, we obtained a virually horizontal line of melting; however, the problems with metastability can, close to the triple point, drastically displace the measured temperatures with respect to the real equilibrium. Additionally, we observed some segregation in the sample, obtained after thermal runs at very high pressures; hence the transition line can be shifted by concentration effects. Our observation corroborates Bridgman's report [11] that pressure can induce partial decomposition of HgTe. These results indicate that further efforts are necessary to determine the cinnabar–liquid coexistence line.

4.2. HgSe

The pressure–temperature ($p-T$) phase diagram of HgSe is characterized by a different pressure dependence (with respect to HgTe) of the melting temperature of the zinc blende phase. It increases from 1070 K at normal pressure to 1093 K for $p = 0.92$ GPa and decreases to 1061 K at the triple point ($p = 1.8$ GPa). The compressibility of the liquid is then much higher than zinc blende. The slope of the melting curve of the cinnabar phase is positive. Similarly, a positive slope is observed for the zinc blende–cinnabar equilibrium line.

The experiments for lower temperatures (zinc blende–cinnabar transition) and higher pressures (cinnabar–liquid) are still required for full determination of the $p-T$ phase diagram of HgSe.

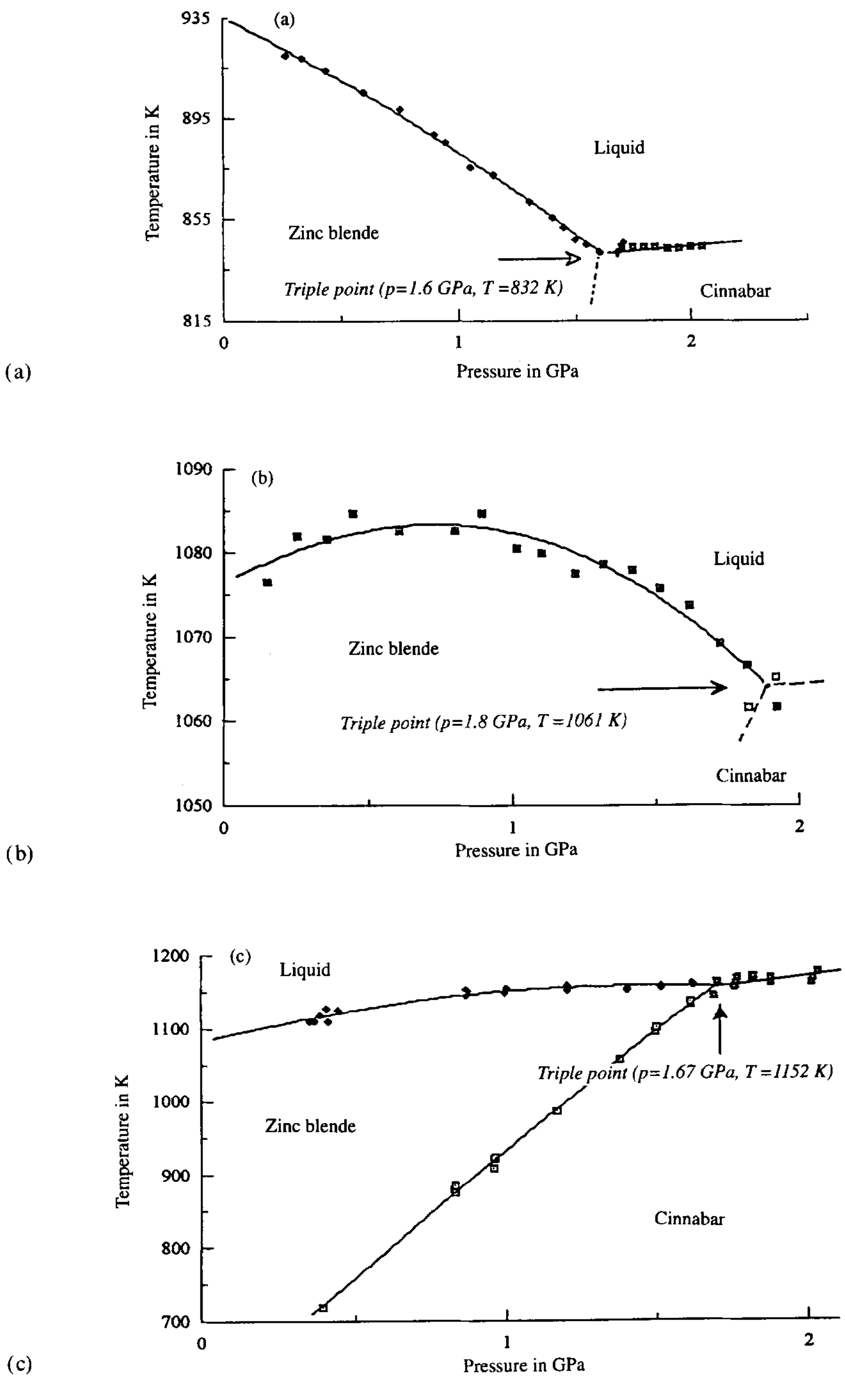

Fig. 6. Pressure–temperature ($p-T$) phase diagrams: (a) HgTe; (b) HgSe; (c) HgS.

4.3. HgS

The pressure–temperature ($p-T$) phase diagrams of HgS (Fig. 6(c)), obtained in our high pressure experiments has the zinc blende–liquid equilibrium line of similar shape to that of HgSe. The melting temperature of the zinc blende at normal pressure, obtained by extrapolation from high pressure results (sublimation of HgS occurs at normal pressure at 853 K), is equal to 1059 K. The melting temperature has its maximum at 1.2 GPa (1160 K) and decreases to 1152 K at the triple point ($p = 1.67$ GPa). Thus the compressibility of the liquid is higher than zinc blende. The zinc blende–cinnabar line is virtually straight ($T = 313 + 369p - 16p^2$) suggesting that compressibilities of both solid phases are either similar or small.

5. Hysteresis in HgS phase transitions

The temperature difference $T_h - T_c$, defined as the difference between the beginning of the transitions for heating and cooling runs as a function of transition pressure and temperature for HgS is presented in Fig. 7(a) and (b) respectively. For melting and solidification it is of the order of 10 K and slowly increases with the transition pressure. The difference $T_h - T_c$ (effectively measured at the same temperature Fig. 7(b)), can be explained by supercooling in the solidification processes and by the kinetic contribution (kinetic shift from the equilibrium temperature). The random nature of the nucleation process in the supercooled melt can also increase the variance of the obtained data.

The magnitude of the temperature difference does not depend on the solid phase structure. Two plausible explanations can be proposed, either the difference is controlled by the kinetic factors in the liquid phase (viscosity, diffusivity, segregation in the interfacial region, etc.) or liquid is supercooled so that the transition to metastable zinc blende occurs and is then followed by transition to the cinnabar phase. In the latter case the hysteresis should be determined by the properties of the liquid–zinc blende transition. At present we cannot determine which mechanism is responsible for the temperature differences.

The cinnabar–zinc blende transition has different properties. Along the $p-T$ coexistence line there is simultaneous change of the temperature and pressure. In spite of considerable variation of temperature (over 500 K) and pressure (1.6 GPa), the difference $T_h - T_c$ is virtually constant. The magnitude of the difference is much greater than for melting/solidification and is equal to about 35 K. Therefore large $T_h - T_c$ values can be attributed to many factors. The solid–solid transition is more difficult to identify (it has small latent heat); however, an error of such magnitude in the identification of the transition temperature has to be excluded. The nucleation barrier should basically depend on the temperature via its temperature dependence which we are not able to estimate. It is most likely that it is the hysteresis mechanism i.e. collective behavior of small crystallites, which impedes the transformation of the neighbors. The transition from zinc blende to cinnabar decreases the volume, which will increase the shear strain around collapsed part of

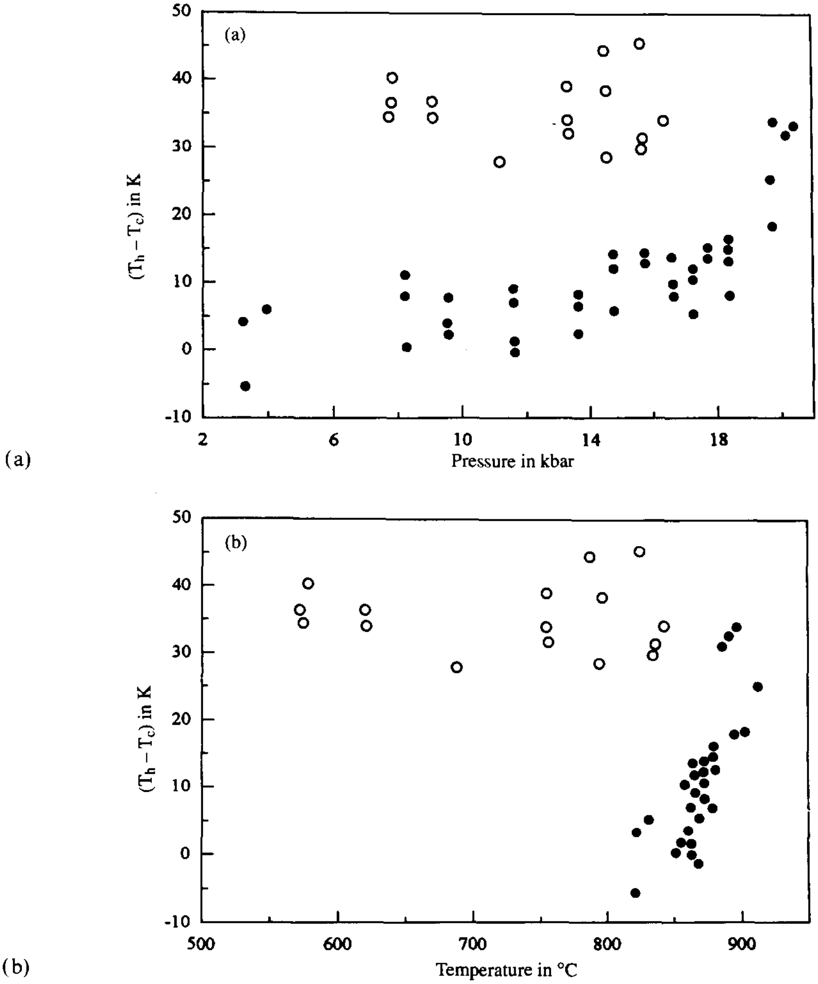

Fig. 7. The temperature difference of the transition peak during heating and cooling: ○, liquid–solid transition; *, solid–solid transition. (a) As a function of pressure; (b) as a function of temperature.

the crystal. Due to the high values of the shear elastic moduli of zinc blende, this configuration can withstand considerable strain, contributing to the supercooling of the zinc blende. We suspect that the considerable strain in zinc blende along with the relatively low mechanical rigidity of cinnabar leads to cracking of the HgS crystals, grown in the zinc blende stability range. This effect was observed first by Curtis in his experiments of crystal growth of HgS from the vapor [13].

Similarly, the transition from cinnabar to zinc blende is accompanied by local increase of the volume, which contributes to volumetric strain in the sample. Locally this can increase the compression and stabilize the cinnabar phase. Hence the transition can be more diffuse, leading to shifts of the measured temperatures of maximal thermal effect. That can also explain the considerable spread of the measured temperature differences (Fig. 7(a) and (b)).

6. Summary and discussion

In this paper we presented $p-T$ diagrams of mercury chalcogenides for pressures up to 2.0 GPa. The triple point coordinates are $p = 1.6$ GPa and $T = 832$ K for HgTe, $p = 1.8$ GPa and $T = 1061$ K for HgSe and $p = 1.66$ GPa and $T = 1152$ K for HgS. The cinnabar–liquid equilibrium line was determined for HgS; its slope is equal to 35.9 K/GPa.

The temperature difference in the melting/solidification transition was found to be small (of the order of 10 K) and slowly increased with pressure. It is probably caused by kinetic factors related to the liquid phase. The difference above the triple point can also be related to the transition to the metastable zinc blende phase. We observed significant variation of the measured temperatures which impede the registration of cinnabar–liquid equilibrium lines. For the zinc blende–cinnabar transition, the hysteresis is much larger (of the order of 35 K) and does not depend on both temperature and pressure. It is probably caused by mechanical factors.

We conclude that further experiments are needed for proper determination of cinnabar–liquid coexistence lines. Special care should be directed towards understanding the mechanism and, when possible, removal of the metastabilities by changing the heating/cooling rates in DTA experiments.

References

[1] A. Werner, H.D. Hochheimer, K. Strossner and A. Jayaraman, Phys. Rev. B, 28 (1983) 3330.
[2] T.-L. Huang and A. Ruoff, Phys. Rev. B, 31 (1985) 5976.
[3] J.A. Kafalas, H.C. Gatos, M.C. Lavine and M.D. Danus, J. Phys. Chem. Solids, 23 (1962) 1591.
[4] A. Jayaraman, W. Klement and G.C. Kennedy, Phys. Rev., 130 (1963) 2277.
[5] J.C. Tedenac, M.C. Record, R.M. Ayral-Marin, G. Brun, J. Jun, I. Grzegory, S. Krukowski and M. Bockowski, Jpn. J. Appl. Phys., 32 (1993) 26.
[6] J.C. Tedenac, M.C. Record, G. Brun, J. Jun, I. Grzegory, O. Vallassiades and D.S. Kyriakos, Semicond. Sci. Technol., 6 (1991) 843.
[7] J.C. Tedenac, R. Astier, J. Jun and I. Grzegory, High Pres. Res., 7–8 (1990) 492.
[8] S. Porowski, J. Jun, S. Krukowski, M. Bockowski, J.C. Tedenac and M.C. Record, J. High Pressure Res.
[9] A.V. Omel'chenko and V.I. Soshnikov, Izv. Ak. Nauk SSSR Neorg. Mater., 18 (1982) 685.
[10] V.I. Sorokin, S.S. Boksha and T.V. Ushakowskaya, Geochimia, 1 (1984) 132.
[11] P.W. Bridgman, Proc. Am. Acad. Arts Sci., 76 (1940) 21.
[12] S. Porowski, J. Jun and I. Grzegory, in J. Jurczak and B. Baranowswki (Eds.), High Pressure Chemical Synthesis, Elsevier, Amsterdam, 1989, p. 21.
[13] O.L. Curtis, Jr, J. Appl. Phys., 33 (1962) 2461.